mixture was stirred and irradiated for several days until the color changed from violet to brown. The solution was then evaporated to dryness, and the residue was extracted with CH_2Cl_2. The solution was chromatographed over Florisil. Elution with hexane/CH_2Cl_2 (2/1) gave a red-brown (M = Mo) or brown (M = W) band, from which the product **10** (M = Mo) or **11** (M = W) was isolated in about 23% (M = Mo) or 40% (M = W) yield. Further elution with CH_2Cl_2 gave the violet starting compound **3**. Complexes **10** and **11** are soluble in common organic solvents are are recrystallized from a CH_2Cl_2/hexane mixture.

Anal. Calcd for $C_{22}H_{16}Mo_4O_{10}S_4$ (**10**): C, 27.8; Mo, 40.3. Found: C, 27.8; Mo, 40.4. Complex **10** decomposed in the mass spectrometer giving the $[(C_5H_5)\overline{Mo(SMe)_4Mo}(C_5H_5)]$ species, suggesting that some recombination took place in the spectrometer. Molar conductivity: 1.5. Anal. Calcd for $C_{17}H_{16}Mo_2O_5S_4W$ (**11**): C, 25.4; S, 15.9; Mo, 23.8; W, 22.8. Found: C, 24.8; S, 15.9; Mo, 21.2; W. 22.0. Molar conductivity: 1.1.

(b) Attempted Dealkylation Reactions of (3). (i) With $[\{(\eta^5\text{-}C_5H_5)Fe(Co)_2\}_2]$ The molybdenum complex **3** (0.8 g, 1.6 × 10^{-3} mol) and excess of $[\{(\eta^5\text{-}C_5H_5)Fe(CO)_2\}_2]$ (0.4 g) were refluxed in toluene for 24 h. Removal of the solvent in vacuo provided only ferrocene and starting complex.

(ii) With $[(\eta^5\text{-}C_5H_5)V(CO)_4]$. Reaction of **3** (0.7 g) in THF with 1 equiv of $[(\eta^5\text{-}C_5H_5)V(CO)_4]$ at 40 °C for 4 days also resulted in no reaction.

(c) Attempted Reaction of 3 with Unsaturated Molecules. Complex **3** (0.8 g, 1.6 × 10^{-3} mol) in tetrahydrofuran was photolyzed or heated for 60 h with 2 × 10^{-3} mol of hexafluorobutyne. After removal of the solvent, only starting complex was detected.

(d) Attempted Reaction of 3 with CO. **3** was dissolved in THF and 1 atm of CO was added. The solution was stirred at 60 °C for 24 h. The starting compound was recovered and identified by IR and NMR spectra.

Acknowledgment. We are grateful to Dr. D. Davies (University of Leicester) for his comments on this paper and to Mr. J. Y. Le Gall for assistance with the NMR. M.B.G-L is indebted to CNPq (Brasil) for a fellowship. We thank the CNRS for financial support.

Registry No. **1a**, 103619-72-3; **1b**, 103667-00-1; **1c** (X = Cl), 103667-03-4; **1c** (X = Br), 103750-97-6; **1d**, 103667-04-5; **1e**, 103667-05-6; **2a**, 103619-73-4; **2b**, 103667-01-2; **3**, 103619-81-4; **5a**, 103639-17-4; **5b**, 103619-76-7; **5c**, 103619-77-8; **6a**, 103639-18-5; **6b**, 103619-78-9; **7a**, 103619-79-0; **7b**, 103619-80-3; **8a**, 81874-19-3; **8b**, 81874-18-2; **9**, 103728-97-8; **10**, 103619-82-5; **11**, 103619-83-6; $[Mo_2(CO)_4(M\text{-}SMe)_2(\eta^5\text{-}C_5H_5)_2]$, 103619-74-5; $[W_2(CO)_4(M\text{-}SMe)_2(\eta^5\text{-}CH_5)_2]$, 103619-75-6; $[Mo(CO)_3Br(\eta^5\text{-}C_5H_5]$, 12079-79-7; $[W(CO)_3Br(\eta^5\text{-}C_5H_5)]$, 37131-50-3; $Na[Fe(CO)_2(\eta^3\text{-}C_5H_5)]$, 12152-20-4; $[\{Fe(CO)_2(\eta^5\text{-}C_5H_5)\}_2]$, 11117-09-2; $Mo(CO)_6$, 13939-06-5; $W(CO)_6$, 14040-11-0; MeSSMe, 624-92-0; sodium acetylide, 1066-26-8.

Supplementary Material Available: A table of anisotropic thermal parameters (1 pages); a listing of structure factor amplitudes (7 pages). Ordering information is given on any current masthead page.

Synthesis, Phosphorus-31 Shift Correlated Two-Dimensional (COSY) Nuclear Magnetic Resonance Spectra, and Structure of the Tris(trimethyl phosphite)-Substituted Phosphido-Bridged Heteronuclear Dimer $[(MeO)_3P]_2(CO)_2Ru(\mu\text{-}PPh_2)Co(CO)_2[P(OMe)_3]$

Salaheddine Guesmi,[†] Nicholas J. Taylor,[‡] Pierre H. Dixneuf,[†] and Arthur J. Carty*[‡]

Laboratoire de Chimie de Coordination Organique, Université de Rennes, Campus de Beaulieu, 35042 Rennes, France, and Guelph-Waterloo Centre for Graduate Work in Chemistry, Waterloo Campus, Department of Chemistry, University of Waterloo, Waterloo, Ontario, Canada N2L 3G1

Received February 25, 1986

Trimethyl phosphite reacts with the phosphido-bridged heterobinuclear complex $(CO)_4Ru(\mu\text{-}PPh_2)Co(CO)_3$ (**1**), affording mono-, $[(MeO)_3P](CO)_3Ru(\mu\text{-}PPh_2)Co(CO)_3$ (**2**), di-, $[(MeO)_3P]_2(CO)_2Ru(\mu\text{-}PPh_2)Co(CO)_3$ (**3a**), and tri-, $[(MeO)_3P]_2(CO)_2Ru(\mu\text{-}PPh_2)Co(CO)_2[P(OMe)_3]$ (**4**), substituted derivatives characterized by microanalysis and infrared and ^1H and ^{31}P NMR spectroscopy. Crystals of **4** are triclinic of space group $P\bar{1}$ with a = 10.240 (2) Å, b = 11.555 (3) Å, c = 16.273 (3) Å, α = 76.24 (2)°, β = 77.97 (2)°, γ = 71.86 (2)°, and $Z = 2$. The crystal structure was solved and refined to R and R_w values of 0.039 and 0.048, respectively, by using 4380 observed ($I \geq 3\sigma(I)$) reflections measured on a Syntex $P2_1$ diffractometer. In the heterobimetallic complex, one trimethyl phosphite ligand is located on the cobalt atom approximately trans to the Ru–Co bond and the two remaining phosphites on the ruthenium, one trans to the Ru–Co bond and the other trans to the phosphido bridge (Ru–P(1)–Co = 76.01 (3)°). An analysis of the ^{31}P NMR spectrum of **4** using two-dimensional (2D) (COSY) techniques has revealed large trans $(MeO)_3P\text{–}PPh_2$ ($^2J_{PPh_2\text{–}P(OMe)_3}$ = 177.4 Hz) and trans $(MeO)_3P\text{–}P(OMe)_3$ ($^3J_{P(OMe)_3\text{–}P(OMe)_3}$ = 80.6 Hz) couplings and much smaller cis coupling constants.

Two fundamental aspects of the rapidly developing chemistry of heterobimetallic complexes[1-11] are the selectivities of the two metal sites for various substrates and the degree to which one metal influences the reactivity patterns of the second center. For saturated 34-electron heterobinuclear carbonyls with strong metal–metal interactions key questions concern the sites and mechanisms (associative or dissociative) of simple substitution reac-

---

[†] Université de Rennes.

[‡] University of Waterloo.

(1) For a recent review of mixed-metal compounds see: (a) Roberts, D. A.; Geoffroy, G. L. In *Comprehensive Organometallic Chemistry*; Wilkinson, G., Stone, F. G. A., Abel, E. W., Eds.; Pergamon: Oxford, 1982, Ch. 40. (b) Langenbach, H. J.; Vahrenkamp, H. *Chem. Ber.* **1979**, *112*, 3773.

(2) Blagg, A.; Cooper, G. R.; Pringle, P. G.; Robson, R.; Shaw, B. L. *J. Chem. Soc., Chem. Commun.* **1984**, 933.

0276-7333/86/2305-1964$01.50/0 © 1986 American Chemical Society

tions.[12] We have previously reported[13] that the phosphido-bridged ruthenium–cobalt compound $(CO)_4Ru(\mu\text{-}PPh_2)Co(CO)_3$ (**1**) reacts site specifically with 1 or 2 mol of phosphines affording mono- and disubstituted derivatives $(L)(CO)_3Ru(\mu\text{-}PPh_2)Co(CO)_3$ (**2**) and $(L)_2(CO)_2Ru(\mu\text{-}PPh_2)Co(CO)_3$ (**3**), respectively. In this paper we describe the reactions of **1** with trimethyl phosphite, $P(OMe)_3$, a ligand known for its ability to cause multiple CO substitutions in carbonyls. In addition to derivatives to types **2** and **3**, a trisubstituted complex, $(L)_2(CO)_2Ru(\mu\text{-}PPh_2)Co(CO)_2(L)$ (**4**) ($L = P(OMe)_3$), has been synthesized and structurally characterized by X-ray crystallography. An analysis of the variable-temperature ^{31}P NMR spectra of **4** ($L = P(OMe)_3$) using two-dimensional (2D) shift correlated (COSY) techniques has provided valuable information on the network of spin–spin-coupled ^{31}P nuclei in phosphorus ligands having different stereochemical dispositions within the heterobinuclear molecule. Such data are likely to be of practical use in structural assignments for other phosphido-bridged polynuclear compounds.

Experimental Section

General Procedures. Standard Schlenk procedures were employed in manipulating air-sensitive materials. Solvents hexane, ether, THF (benzophenone ketyl), and dichloromethane (P_2O_5) were dried in the usual fashion and distilled prior to usage. Chromatographic separations used Florisil (columns) or Merck silica gel (plates).

Instrumentation. Infrared spectra were recorded on Perkin-Elmer 983, Perkin-Elmer 180, and Perkin-Elmer 225 instruments using matched sodium chloride cells of path length 0.5 mm. Mass spectra were recorded at the Centre de Mêsures Physiques de l'Ouest, Universitê de Rennes, with a Varian MAT-311 double-focusing mass spectrometer operating at 70 eV. Routine ^1H and $^{31}P\{^1H\}$ NMR spectra were measured on Bruker WP-80 spectrometers at 80 MHz for ^1H and 32.38 MHz for ^{31}P. Higher field $^{31}P\{^1H\}$ spectra were recorded on a Bruker AM-250 system at 101.2 MHz in 10-mm tubes with CD_2Cl_2 as the solvent and lock. Homonuclear ^{31}P-shift correlated 2D NMR (COSY) experiments were conducted at 101.2 (Bruker AM-250) and 121.5 MHz (Bruker AM-300) on solutions containing ~300 mg of complex. All ^1H shifts are referenced to Me_4Si ($\delta = 0$) and ^{31}P shifts to 85% H_3PO_4.

Synthesis. $\mathbf{[(MeO)_3P](OC)_3Ru(\mu\text{-}PPh_2)Co(CO)_3}$ **(2a,b) and** $\mathbf{[(MeO)_3P]_2(OC)_2Ru(\mu\text{-}PPh_2)Co(CO)_3}$ **(3a).** A solution of **1**[14] (0.5 g; 0.92 mmol) and an excess of $P(OMe)_3$ (0.2 mL; 1.7 mmol) in 60 mL of THF was heated for 12 h at 45 °C. After filtration of the reaction mixture on a frit and evaporation of the solvent, the products were chromatographed on a column (3 × 20 cm) of silica gel. Elution first with hexane afforded the red complexes **2a,b** (0.65 g, 11%) and then with hexane–CH_2Cl_2 (4/1) gave the red derivative **3a** (0.27 g, 39%). Final elution with dichloromethane gave only traces of **4**.

Table I: Crystal Data, Intensity Collection, Reduction, and Refinement for $\mathbf{[(MeO)_3P]_2(CO)_2Ru(\mu\text{-}PPh_2)Co(CO)_2[P(OMe)_3]}$

formula	$RuCoP_4O_{13}C_{25}H_{37}$
mol wt	829.46
cryst class	triclinic
space group	$P\bar{1}$
a, Å	10.240 (2)
b, Å	11.555 (3)
c, Å	16.273 (3)
α, deg	76.24 (2)
β, deg	77.97 (2)
γ, deg	71.86 (2)
V, Å^3	1758.2
Z	2
ρ_{measd}, g cm^{-3}	1.58
ρ_{calcd}, g cm^{-3}	1.567
$F(000)$	844
μ(Mo Kα), cm^{-1}	11.50
cryst size, mm	0.29 × 0.33 × 0.35
transmisn factors	0.62–0.77
radiatn	Mo Kα (λ = 0.71069 Å)
max 2θ, deg	46.0
scan speed, deg min^{-1}	variable; 2.93–29.3
scan width, deg	0.8 below Kα_1 to 0.8 above Kα_2
stds (every 100 measurements)	109, 532
T, K	293 ± 1
reflctns measd	4928
reflctns obsd	4380
R(isotropic)	0.087
R(anisotropic)	0.053
final R	0.039
R_w	0.048
w^{-1}	$3.9 - 0.0788\lvert F_0\rvert + 0.00153\lvert F_0\rvert^2$
max residuals, e Å^{-3}	0.78

2a,b: mp 96–98 °C; IR (Nujol) 2093 (m), 2026 (vs), 1989 (vs), 1939 (s) 1927 (vs), 1894 (w) cm^{-1}; ^{31}P NMR (CD_2Cl_2, 193 K, 32.38 MHz), **2a**, δ 177.8 (s, μ-PPh_2), 147.4 (s, $P(OMe)_3$), **2b**, δ 181.8 (d, μ-PPh_2), 148.5 [d, $P(OMe)_3$, $^2J_{P_\mu-P(eq,trans)} = 173$ Hz].

3a: mp 164–165 °C; IR (Nujol) 2069 (w), 1983 (vs), 1971 (vs), 1927 (s), 1907 (s) cm^{-1}. ^{31}P NMR (CD_2Cl_2, 193 K, 32.38 MHz) δ 173 [d, μ-PPh_2, $^2J_{P_\mu-P(eq,trans)} = 188$ Hz], 150 [dd, eq,trans-$P(OMe)_3$], 151 [d, eq,cis-$P(OMe)_3$, $^2J_{P(eq,cis)-P(eq,trans)} = 22$ Hz].

$\mathbf{[(MeO)_3P]_2(OC)_2Ru(\mu\text{-}PPh_2)Co(CO)_2[P(OMe)_3]}$ **(4). From 1.** A solution of **1** (0.54 g, 1 mmol) and 3 equiv of $P(OMe)_3$ (0.35 mL, 3 mmol) in THF (60 mL) was refluxed for 12 h. After filtration of the solution on a frit and evaporation of solvent, the residue was extracted with ether (30 mL). The red complex **4** crystallized from this solution (0.7 g, 85%).

From 3a. A solution of **3a** (0.73 g, 1 mmol) and an excess of $P(OMe)_3$ (0.77 mL, 7.5 mmol) in THF (60 mL) was refluxed for 12 h. The solution was filtered on a frit, the THF was evaporated, and the red complex was extracted with ether (30 mL) from which it crystallized (0.63 g, 76%): mp 134–136 °C; IR (Nujol) 2037 (m), 1972 (br), 1921 (vs), 1876 (s) cm^{-1}; ^1H NMR ($CDCl_3$, 303 K, 100 MHz) δ 1.04–7.54 (m, C_6H_5), 3.72 (d), 3.40 (d), 3.38 (d, $^3J_{PH} = 12$ Hz); ^{31}P NMR (CD_2Cl_2, 193 K, 101.2 MHz), see Table IV. Anal. Calcd for $C_{25}H_{37}O_{13}P_4CoRu$: C, 36.20; H, 4.49; P, 14.93. Found: C, 36.19; H, 4.41; P, 14.70.

X-ray Analysis: Crystallographic Data, Collection, and Reduction. Single crystals of **4** were grown from hexane/dichloromethane solutions at −5 °C. A suitable crystal of dimensions 0.29 × 0.33 × 0.35 mm was glued to a glass fiber and mounted on a eucentric goniometer head for preliminary space group determination and unit cell measurement. The crystal was centered on a $P2_1$ automated diffractometer and the Syntex axial photograph, autoindexing, and cell refinement routines used to determine accurate unit cell parameters. An inspection of diffraction data revealed no systematic absences and triclinic symmetry. Intensity data were collected as indicated in Table I by using Mo Kα radiation. Intensities of two standard reflections, monitored after every 100 measurements, showed only minor fluctuations

---

(3) Warner, K. E.; Norton, J. R. *Organometallics* **1985**, *4*, 2150.

(4) Casey, C. P.; Bullock, R. M. *Organometallics* **1984**, *3*, 1100.

(5) Mercer, W. C.; Geoffroy, G. L.; Rheingold, A. L. *Organometallics* **1985**, *4*, 1418.

(6) Chaudret, B.; Dahan, F.; Saba, S. *Organometallics* **1985**, *4*, 1490.

(7) MacLaughlin, S. A.; Murray, R. C.; Dewan, J. C.; Schrock, R. R. *Organometallics* **1985**, *4*, 796.

(8) Guesmi, S.; Süss-Fink, G.; Dixneuf, P. H.; Taylor, N. J.; Carty, A. J.; *J. Chem. Soc., Chem. Commun.* **1984**, 1606. Regragui, R.; Dixneuf, P. H.; Taylor, N. J.; Carty, A. J. *Organometallics* **1984**, *3*, 814.

(9) Delavaux, B.; Chaudret, B.; Dahan, F.; Poilblanc, R. *Organometallics* **1985**, *4*, 935.

(10) Horton, A. D.; Mays, M. J.; Raithby, P. R. *J. Chem. Soc., Chem. Commun.* **1985**, 247.

(11) Mercer, W. C.; Whittle, R. R.; Burkhardt, E. W.; Geoffroy, G. L. *Organometallics* **1985**, *4*, 68.

(12) (a) Fawcett, J. P.; Poe, A. J. *J. Chem. Soc., Dalton Trans.* **1976**, 2039. (b) Sonnenberger, D.; Atwood, J. D. *J. Am. Chem. Soc.* **1980**, *102*, 3484. (c) Fawcett, J. P.; Poe, A. J.; Sharma, K. R. *J. Am. Chem. Soc.* **1976**, *98*, 1401.

(13) Regragui, R.; Dixneuf, P. H.; Taylor, N. J.; Carty, A. J. *Organometallics* **1986**, *5*, 1.

(14) Regragui, R.; Dixneuf, P. H. *J. Organomet. Chem.* **1982**, *239*, C12. Regragui, R.; Dixneuf, P. H.; Taylor, N. J.; Carty, A. J. *Organometallics* **1984**, *3*, 1020.

Table II. Atomic Positional Parameters (Fractional × 10^4) for $[P(OMe)_3]_2(CO)_2Ru(\mu\text{-}PPh_2)Co(CO)_2[P(OMe)_3]$

atom	*x*	*y*	*z*
Ru	6691.1 (4)	5921.2 (3)	2416.2 (2)
Co	4344.7 (6)	7036.9 (6)	2504.8 (4)
P(1)	6445.9 (13)	7087.4 (11)	2487.7 (8)
P(2)	8994.5 (15)	4141.0 (13)	2392.9 (10)
P(3)	6061.9 (14)	3331.8 (12)	2290.2 (8)
P(4)	3270.4 (14)	8814.6 (12)	2739.5 (9)
O(1)	6986 (4)	5874 (4)	478 (2)
O(2)	6014 (5)	4304 (4)	4365 (2)
O(3)	3542 (6)	7413 (5)	829 (3)
O(4)	2820 (5)	5669 (5)	3899 (3)
O(5)	9720 (4)	4900 (4)	2710 (4)
O(6)[a]	9643 (6)	2730 (5)	2683 (4)
O(6A)[b]	9406 (13)	3119 (13)	3378 (8)
O(7)[a]	9940 (6)	4248 (6)	1409 (4)
O(7A)[b]	9950 (10)	3263 (11)	1850 (7)
O(8)	7240 (4)	2537 (3)	1681 (3)
O(9)	5872 (4)	2309 (3)	3115 (2)
O(10)	4657 (4)	3479 (3)	1945 (2)
O(11)	1627 (4)	9189 (4)	2927 (4)
O(12)	3611 (4)	9895 (3)	2008 (3)
O(13)	3498 (5)	9310 (4)	3531 (3)
C(1)	6866 (5)	5560 (4)	1197 (3)
C(2)	6261 (5)	4598 (5)	3646 (3)
C(3)	3907 (6)	7232 (5)	1290 (4)
C(4)	3460 (6)	6185 (5)	3361 (4)
C(5)	11210 (8)	4551 (9)	2758 (8)
C(6)	9181 (8)	2065 (8)	3555 (5)
C(7)	10011 (8)	3539 (8)	852 (5)
C(8)	7098 (9)	1440 (6)	1440 (5)
C(9)	4584 (7)	2404 (7)	3705 (4)
C(10)	4394 (8)	4186 (7)	1101 (4)
C(11)	782 (7)	8759 (9)	2555 (6)
C(12)	2957 (8)	11198 (6)	2023 (5)
C(13)	3431 (9)	8588 (8)	4358 (4)
C(14)	7063 (5)	7482 (5)	3343 (3)
C(15)	6825 (6)	8738 (5)	3349 (4)
C(16)	7284 (7)	9101 (6)	3971 (4)
C(17)	7950 (7)	8224 (7)	4598 (4)
C(18)	8186 (8)	6964 (7)	4601 (4)
C(19)	7722 (6)	6607 (5)	3975 (4)
C(20)	7337 (5)	7933 (4)	1544 (3)
C(21)	8765 (6)	7754 (5)	1460 (4)
C(22)	9468 (7)	8327 (6)	727 (4)
C(23)	8726 (8)	9094 (6)	86 (4)
C(24)	7299 (7)	9291 (5)	166 (4)
C(25)	6604 (6)	8698 (5)	904 (3)

[a] Occupancy = $^2/_3$. [b] Occupancy = $^1/_3$.

(±1%). Data were corrected for Lorentz and polarization effects and then converted to unscaled $|F_o|$ values. No absorption correction was needed.

Solution and Refinement of the Structure. All calculations were carried out on a system of programs described elsewhere[15] using an IBM 4341 network in the University of Waterloo Computing Centre. Neutral atom scattering factors were taken from the ref 16; both real ($\Delta F'$) and imaginary ($\Delta F''$) components of anomalous dispersion for ruthenium and cobalt were included. The function minimized in least-squares refinement was $\sum w(\Delta|F|)^2$.

Table III. Bond Lengths (Å) and Angles (deg) for $[P(OMe)_3]_2(CO)Ru(\mu\text{-}PPh_2)Co(CO)_2[P(OMe)_3]$

(a) Bond Lengths

Ru–CO	2.7837 (7)	Ru–P(1)	2.350 (1)
Ru–P(2)	2.255 (2)	Ru–P(3)	2.301 (1)
Ru–C(1)	1.920 (5)	Ru–C(2)	1.934 (5)
Co–P(1)	2.165 (1)	Co–P(4)	2.090 (2)
Co–C(3)	1.747 (6)	Co–C(4)	1.763 (6)
P(1)–C(14)	1.842 (5)	P(2)–C(20)	1.845 (5)
P(2)–O(5)	1.539 (5)	P(2)–O(6)	1.554 (6)
P(2)–O(7)	1.688 (7)	P(2)–O(6A)	1.792 (14)
P(2)–O(7A)	1.488 (12)	P(3)–O(8)	1.589 (4)
P(3)–O(9)	1.586 (4)	P(3)–O(10)	1.598 (5)
P(4)–O(11)	1.583 (5)	P(4)–O(12)	1.578 (4)
P(4)–O(13)	1.612 (5)	C(1)–O(1)	1.133 (6)
C(2)–O(2)	1.135 (6)	C(3)–O(3)	1.162 (8)
C(4)–O(4)	1.144 (8)	O(5)–C(5)	1.466 (10)
O(6)–C(6)	1.502 (11)	O(6A)–C(6)	1.264 (17)
O(7)–C(7)	1.346 (10)	O(7A)–C(7)	1.571 (14)
O(8)–C(8)	1.468 (8)	O(9)–C(9)	1.451 (8)
O(10)–C(10)	1.452 (8)	O(11)–C(11)	1.410 (10)
O(12)–C(12)	1.448 (7)	O(13)–C(13)	1.405 (9)
C(14)–C(15)	1.397 (8)	C(15)–C(16)	1.394 (9)
C(16)–C(17)	1.379 (10)	C(17)–C(18)	1.399 (10)
C(18)–C(19)	1.400 (9)	C(19)–C(14)	1.380 (8)
C(20)–C(21)	1.393 (9)	C(21)–C(22)	1.395 (9)
C(22)–C(23)	1.387 (10)	C(23)–C(24)	1.390 (11)
C(24)–C(25)	1.405 (8)	C(25)–C(20)	1.380 (8)

(b) Bond Angles

Co–Ru–P(1)	48.99 (3)	Co–Ru–P(2)	151.86 (4)
Co–Ru–P(3)	109.44 (3)	Co–Ru–C(1)	86.6 (2)
Co–Ru–C(2)	86.5 (2)	P(1)–Ru–P(2)	103.89 (5)
P(1)–Ru–P(3)	158.27 (4)	P(1)–Ru–C(1)	86.3 (2)
P(1)–Ru–C(2)	91.3 (2)	P(2)–Ru–P(3)	98.69 (5)
P(2)–Ru–C(1)	93.2 (2)	P(2)–Ru–C(2)	94.3 (2)
P(3)–Ru–C(1)	90.1 (2)	P(3)–Ru–C(2)	89.5 (2)
C(1)–Ru–C(2)	172.5 (2)	Ru–Co–P(1)	55.01 (3)
Ru–Co–P(4)	153.50 (4)	Ru–Co–C(3)	99.2 (2)
Ru–Co–C(4)	92.1 (2)	P(1)–Co–P(4)	99.32 (5)
P(1)–Co–C(3)	113.8 (2)	P(1)–Co–C(4)	122.8 (2)
P(4)–Co–C(3)	97.6 (2)	P(4)–Co–C(4)	98.4 (2)
C(3)–Co–C(4)	117.1 (3)	Ru–P(1)–Co	76.01 (3)
Ru–P(1)–C(14)	121.7 (2)	Ru–P(1)–C(20)	114.3 (2)
Co–P(1)–C(14)	125.3 (2)	Co–P(1)–C(20)	120.3 (2)
C(14)–P(1)–C(20)	99.7 (2)	Ru–P(2)–O(5)	113.2 (2)
Ru–P(2)–O(6)	123.4 (2)	Ru–P(2)–O(7)	114.8 (2)
Ru–P(2)–O(6A)	112.4 (4)	Ru–P(2)–O(7A)	128.7 (5)
O(5)–P(2)–O(6)	110.7 (3)	O(5)–P(2)–O(7)	93.7 (3)
O(6)–P(2)–O(7)	96.0 (3)	O(5)–P(2)–O(6A)	81.1 (5)
O(5)–P(2)–O(7A)	113.9 (5)	O(6A)–P(2)–O(7A)	94.0 (6)
Ru–P(3)–O(8)	110.1 (1)	Ru–P(3)–O(9)	119.1 (1)
Ru–P(3)–O(10)	121.9 (1)	O(8)–P(3)–O(9)	101.6 (2)
O(8)–P(3)–O(10)	104.1 (2)	O(9)–P(3)–O(10)	97.3 (2)
Co–P(4)–O(11)	119.2 (2)	Co–P(4)–O(12)	114.2 (2)
Co–P(4)–O(13)	121.7 (2)	O(11)–P(4)–O(12)	104.1 (3)
O(11)–P(4)–O(13)	96.4 (3)	O(12)–P(4)–O(13)	97.4 (2)
Ru–C(1)–O(1)	179.1 (2)	Ru–C(2)–O(2)	177.4 (2)
Co–C(3)–O(3)	175.9 (3)	Co–C(4)–O(4)	176.2 (3)
P(2)–O(5)–C(5)	124.8 (4)	P(2)–O(6)–C(6)	121.0 (3)
P(2)–O(6A)–C(6)	120.4 (4)	P(2)–O(7)–C(7)	123.5 (4)
P(2)–O(7A)–C(7)	122.1 (4)	P(3)–O(8)–C(8)	122.6 (3)
P(3)–O(9)–C(9)	123.0 (3)	P(3)–O(10)–C(10)	121.0 (3)
P(4)–O(11)–C(11)	124.3 (4)	P(4)–O(12)–C(12)	123.7 (3)
P(4)–O(13)–C(13)	120.3 (4)		
P(1)–C(14)–C(15)	117.4 (3)	P(1)–C(14)–C(19)	123.5 (3)
C(19)–C(14)–C(15)	119.1 (3)	C(14)–C(15)–C(16)	120.4 (4)
C(15)–C(16)–C(17)	120.4 (4)	C(16)–C(17)–C(18)	119.7 (4)
C(17)–C(18)–C(19)	119.5 (4)	C(18)–C(19)–C(14)	120.8 (4)
P(1)–C(20)–C(21)	119.8 (2)	P(1)–C(20)–C(25)	120.2 (2)
C(25)–C(20)–C(21)	120.0 (3)	C(20)–C(21)–C(22)	120.5 (4)
C(21)–C(22)–C(23)	119.2 (4)	C(22)–C(23)–C(24)	120.9 (4)
C(23)–C(24)–C(25)	119.5 (4)	C(24)–C(25)–C(20)	120.0 (3)

The structure was solved by standard Patterson and Fourier techniques using the full set of 4380 observed ($I \geq 3\sigma(I)$) reflections. Following location of the ruthenium and cobalt atoms in a Patterson map, subsequent Fourier syntheses revealed all non-hydrogen atom positions. Refinement of positions and isotropic temperature factors gave an *R* value ($R = \sum||F_o| - |F_c||/\sum|F_o|$) of 0.087. Conversion to anisotropic coefficients and refinement reduced *R* to 0.053. At this stage a difference Fourier synthesis revealed a disorder of one trimethyl phosphite ligand with clear resolution of oxygen atoms O(6) and O(7) into two centers of electron density. In subsequent cycles these two sites were refined with occupancy factors of $^2/_3$ and $^1/_3$. Convergence was achieved at $R = 0.039$ with the weighted residual $R_w = 0.048$ ($R_w = [\sum w||F_o| - |F_c||^2/\sum w|F_o|^2]^{1/2}$). A weighting scheme of the form $w^{-1} = 3.9 - 0.0788|F_o| + 0.001\,53|F_o|^2$ was employed in the

---

(15) Carty, A. J.; Mott, G. N.; Taylor, N. J.; Yule, J. E. *J. Am. Chem. Soc.* **1978**, *100*, 3051.

(16) *International Tables for X-ray Crystallography*; Kynoch Press: Birmingham, England, 1974; Vol. IV.

Table IV. ^{31}P Chemical Shifts and Coupling Constants for $[(MeO)_3P](CO)_3Ru(\mu\text{-}PPh_2)Co(CO)_3$ (2),[a] $[(MeO)_3P]_2(CO)_2Ru(\mu\text{-}PPh_2)Co(CO)_3$ (3),[a] and $[(MeO)_3P]_2(CO)_2Ru(\mu\text{-}PPh_2)Co(CO)_2[P(OMe)_3]$ (4)[b]

	δ				J, Hz					
	P_1	P_2	P_3	P_4	$^2J_{P_1-P_2}$	$^2J_{P_1-P_3}$	$^2J_{P_1-P_4}$	$^2J_{P_2-P_3}$	$^3J_{P_2-P_4}$	$^3J_{P_3-P}$
cis isomer **2a**	177.8	147.4								
trans isomer **2b**	181.8		148.5			173				
3a	173	151	150			188		22		
4	149	154.9	157.4	191.6	11.5	177.4	39.7	17.22	80.6	

[a] In $CDCl_3$. [b] In toluene-d_8.

Scheme I $[L = P(OMe)_3]$

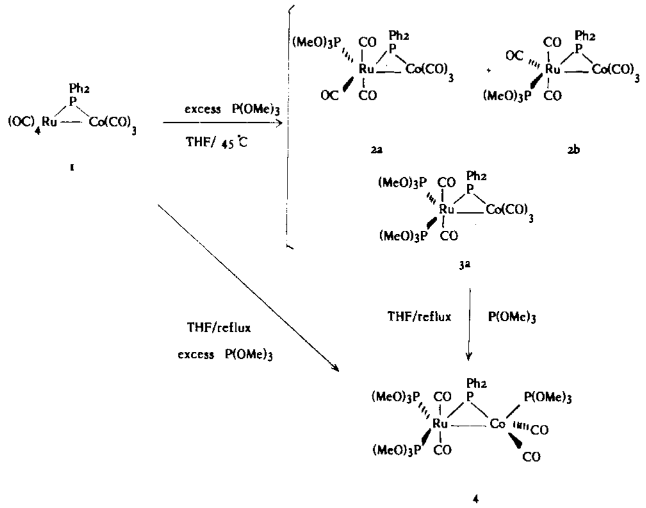

last cycles of refinement. A final difference map exhibited maximum residuals of 0.78 e Å^{-3}. All refinements utilized the full matrix. Table II lists atomic positional parameters and Table III bond lengths and angles. Thermal parameters (Table S1) and structure factor amplitudes (Table S2) have been deposited as supplementary material.

Results and Discussion

Synthesis. The study of site selectivity in carbonyl substitution of the bimetallic system 1 by phosphine ligands led us[13] to the following conclusions: (i) substitution takes place only at the Ru site; (ii) weak donor phosphines (arylphosphines) favor the formation of monosubstituted products of type 2, $L(OC)_3Ru(\mu\text{-}PPh_2)Co(CO)_3$, whereas with basic phosphines(PMe_2Ph, PMe_3) or secondary phosphines (Ph_2PH) the reactions proceeded to the disubstituted derivatives $L_2(OC)_2Ru(\mu\text{-}PPh_2)Co(CO)_3$ of type 3. In an attempt to examine how a weak donor phosphorus derivative with a small cone angle would modify this result, we reacted complex 1 with $P(OMe)_3$, a ligand which is also known to form strong metal–phosphorus bonds. An excess of $P(OMe)_3$ was reacted with 1 in THF, and the reaction was monitored by thin-layer chromatography. At room temperature no significant reaction was observed. When the reaction mixture was heated from 45 °C to reflux in THF, the formation of three types of complex was observed. At 45 °C for 12 h two red products were formed which were separated by column chromatography and identified as the monosubstituted complex 2 (11%) and the disubstituted derivative 3 (Scheme I). On continued refluxing complexes 2 and 3 slowly disappeared, and after 12 h only a third red complex was present which was obtained by crystallization in ether in 85% yield and identified as the trisubstituted derivative 4 (Scheme I). The same complex 4 was also obtained in larger yield (76%) by reacting the disubstituted complex **3a** with an excess of $P(OMe)_3$ in THF at reflux (12 h). These reactions thus suggest that (i) mono- and disubstitution at the Ru site is favored over substitution at cobalt and (ii) disubstitution at the Ru site appears to be necessary prior to substitution at cobalt.

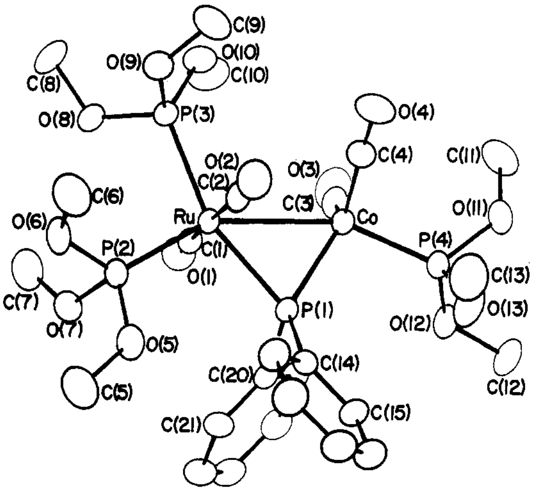

Figure 1. The molecular structure of $[(MeO)_3P]_2(CO)_2Ru(\mu\text{-}PPh_2)Co(CO)_2[P(OMe)_3]$ showing the atomic numbering.

Complexes 2 and **3a** possess phosphite groups bonded only to the ruthenium atom as indicated by ^{31}P NMR (Table IV). Complex 2 contains both cis (**2a**) and trans (**2b**) isomers. The coupling constant $^2J_{(PPh_2)P-[(MeO)_3P)P}$ was observed only for the trans isomer **2b**. Comparison of the ^{31}P NMR spectra of **3a** with those of other $(L)_2(CO)_2Ru(\mu\text{-}PPh_2)Co(CO)_3$ derivatives[13] establishes conclusively that **3a** has a structure with two phosphites bonded to ruthenium in the equatorial plane respectively trans and cis to the PPh_2 group. Phosphorus–phosphorus coupling constants are, as expected, somewhat larger in the phosphite derivative. The ^{31}P NMR spectrum of 4 will be discussed later.

Description and Discussion of the Structure of 4. A view of the molecule, looking down on the Ru–Co–P(1) plane, is illustrated in Figure 1. The two metal atoms are linked by a single diphenylphosphido bridge (Ru–P(1)–Co = 76.01 (3)°), and the Ru–Co distance of 2.7837 (7) Å is consistent with the presence of a strong metal–metal interaction. For comparison Ru–Co bond lengths in the related phosphido-bridged compounds $(PPh_3)(CO)_3Ru(\mu\text{-}PPh_2)Co(CO)_3$[13] and $(PPh_3)(CO)_3Ru(\mu\text{-}PPh_2)Co(CO)_2(PPh_3)$[17] are 2.7681 (4) and 2.750 (1) Å, respectively. In the present context the principal structural features of interest are the stereochemistries of the ruthenium and cobalt atoms and the locations of the three phosphite ligands. Although no structural data are available for the parent molecule $(CO)_4Ru(\mu\text{-}PPh_2)Co(CO)_3$,[14] the structure of 4 ($L = P(OMe)_3$) can be clearly related to that of the monosubstituted triphenylphosphine complex 2 ($L = PPh_3$).[13] In the latter molecule the stereochemistry of the ruthenium atom is that of a distorted octahedron with the phosphorus atom of the phosphine approximately trans

---

(17) Foley, H. C.; Finch, W. C.; Pierpont, C. G.; Geoffroy, G. L. *Organometallics* **1982**, *1*, 1379.

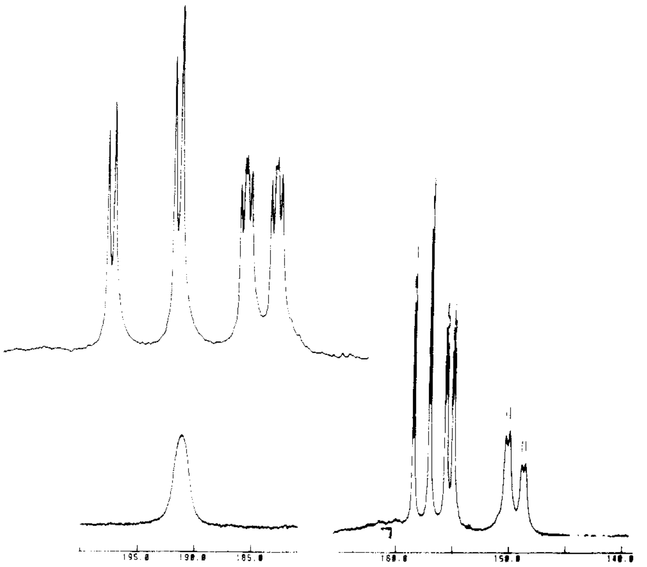

Figure 2. The ^{31}P NMR spectrum of $[(MeO)_3P]_2(CO)_2Ru(\mu\text{-}PPh_2)Co(CO)_2[P(OMe)_3]$ (4) at 297 K. The assignments refer to phosphorus nuclei labeled as in Figure 1.

to the Ru–Co vector and cis to the phosphido bridge. In 4, Ru, Co, and the three phosphorus atoms P(1), P(2), and P(3) define an approximate square plane with C(1)–P(1) and C(2)–O(2), respectively, below and above this plane. The phosphite atom P(2) occupies a similar position trans to the Ru–Co bond (P(2)–Ru–Co = 151.86 (4)°) as PPh_3 in 2 (L = PPh_3) with the second phosphite trans to the phosphido-bridge (P(1)–Ru–P(3) = 158.27 (4)°). The two phosphite ligands are thus cis to one another in the ruthenium coordination sphere (P(2)–Ru–P(3) = 98.69 (5)°). The cobalt atom has a very distorted five-coordinate stereochemistry similar to that in 2 (L = PPh_3) but with one of the basal carbonyl groups in 2, that trans to the Co–Ru bond, substituted by the third phosphite ligand. Although the atoms P(2), Ru, Co, and P(4) are by no means colinear, the phosphites P(2) and P(4) are mutually trans to the Ru–Co bond, a fact which appears to be substantiated by the magnitude of the three-bond P–P coupling in the ^{31}P spectra of 4. There is an interesting comparison of Ru–P bond lengths between 2 (L = PPh_3) and 4 (L = $P(OMe)_3$). In the triphenylphosphine derivative 2, the Ru–P(PPh_3) distance is 2.410 (3) Å, 0.155 Å longer than the corresponding distance (Ru–P(2) = 2.255 (2) Å in the phosphite complex 4. We have previously commented on the fact that in comparable stereochemical situations, M–P(phosphite) bond lengths are consistently shorter, at the level of 0.05–0.11 Å, than M–P(phosphine) bonds and provided possible explanations for this observation.[18] In the present case, the comparison is not a precise one due to the differing degrees of substitution in 2 and 4; nevertheless, this difference (0.155 Å) and the shortness of Ru–P(2) in 4 when compared to the sum of the covalent radii for phosphorus (1.10 Å) and ruthenium (~1.40 Å) suggest that the phosphite is very strongly bound to the ruthenium atom. The second phosphite on ruthenium exhibits a somewhat longer Ru–P bond length (Ru–P(3) = 2.301 (1) Å) probably as a result of the high trans influence of the μ-PPh_2 group. For the phosphite coordinated to cobalt in 4 comparison with the X-ray data for $(PPh_3)(CO)_3Ru(\mu\text{-}PPh_2)Co(CO)_2(PPh_3)$[17] elicits similar conclusions regarding the length of the Co–P bonds, with the Co–$P(OMe)_3$ distance (2.090 (2) Å) significantly shorter

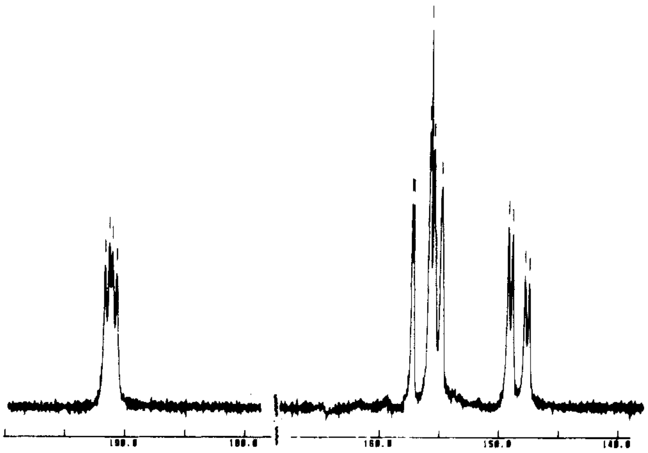

Figure 3. The ^{31}P NMR spectrum of $[(MeO)_3P]_2(CO)_2Ru(\mu\text{-}PPh_2)Co(CO)_2[P(OMe_3)]$ (4) at 233 K.

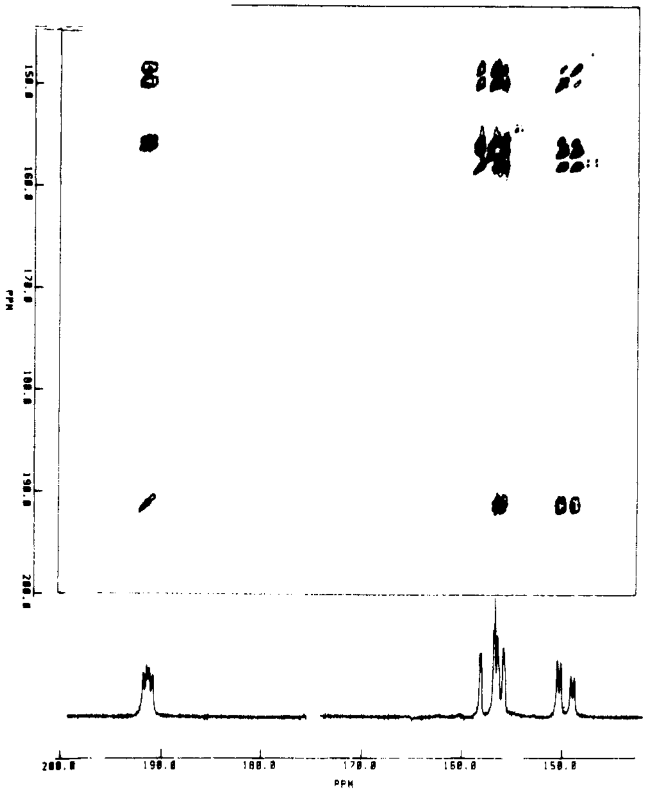

Figure 4. A 2D COSY plot of the ^{31}P NMR spectrum of $[(MeO)_3P]_2(CO)_2Ru(\mu\text{-}PPh_2)Co(CO)_2[P(OMe)_3]$ (4). Diagonal elements represent chemical shifts and off-diagonal elements ^{31}P nuclei related by scalar coupling.

than either the Co–PPh_3 bond length (2.167 (3) Å) or the Co–PPh_2 (2.165 (1) Å) distance in 4.

^{31}P NMR Studies of $[P(OMe)_3]_2(CO)_2Ru(\mu\text{-}PPh_2)Co(CO)_2[P(OMe)_3]$ (4). In a previous study we reported the complex ^{31}P NMR spectrum of 3 (L = PPh_2H), a molecule which exists in solution as a mixture of four geometrical isomers differing in stereochemistry at the quasioctahedral ruthenium atom.[13] A satisfactory interpretation of the spectra of 3 (L = PPh_2H) was achieved by using high-field ^{31}P NMR and 2D COSY techniques. We have now applied these methods to 4 (L = $P(OMe)_3$), a molecule which might be predicted from the ORTEP plot of Figure 1 to present a second-order ABXM spin system. At 32.38 MHz the $^{31}P\{^1H\}$ spectrum is complex. Greater detail is evident at 121.5 MHz (Figure 2), and a full analysis is possible from spectra at lower temperatures (Figure 3) in conjunction with a COSY experiment which

---

(18) Robert, P.; LeBozec, H.; Dixneuf, P. H.; Hartstock, F.; Taylor, N. J.; Carty, A. J. *Organometallics*, **1982**, *1*, 1148.

reveals all of the scalar P–P couplings (Figure 4). In the following discussion phosphorus nuclei are numbered according to Figure 1.

At ambient temperature the 121.5-MHz spectrum (Figure 2) shows a broad unresolved downfield resonance at 190.52 ppm, a pair of doublets at 158.13 and 156.70 ppm, a pair of doublets at 155.23 and 154.58 ppm, and a pair of broad doublets at 149.74 and 148.31 ppm. Although at first sight it might be assumed that the low-field signal arises from the μ-PPh$_2$ group, variable-temperature studies show that this resonance broadens and collapses faster than the high-field doublet of doublets as the temperature is raised. This line broadening can be attributed to the quadrupolar effects of the ^{59}Co ($I = {}^7/_2$) nucleus. Moreover at low temperatures (Figure 3) additional fine structure is resolved in the high-field doublets, whereas the low-field signal remains as a doublet of doublets. We assign the low-field resonance to the phosphite bound to cobalt (P4) and the high-field resonances to P(1) of the phosphido group. Although the high-field resonance signal appears as a doublet of doublets (Figure 3), the COSY spectrum (Figure 4) indicates that the corresponding ^{31}P nucleus P(1) is coupled to three other phosphorus nuclei, P(2), P(3), and P(4). The COSY spectrum also shows that P(2) is coupled to three other phosphorus nuclei, P(2), P(3), and P(4), P(2) is coupled with P(1), P(3), and P(4), P(3) is coupled only to P(1) and P(2), and P(4) is coupled to P(1) and P(2). A complete analysis of shifts and coupling constants is given in Table IV.

There are several notable features of this assignment: (i) $^2J_{\mathrm{P(1)-P(3)}}$ is large (177.4 Hz) as expected for two trans related ligands. Trans $^2J_{\mathrm{P-P(\mu-PPh_2)}}$ values in **3** (L = PPh$_3$H)[13] and (L)(CO)$_2$Ru(μ-PPh$_2$)(μ-C≡C-*i*-Pr)Ru(CO)$_3$ (L = Ph$_2$PC≡C-*i*-Pr)[19] are 183 and 215 Hz, respectively; (ii) $^3J_{\mathrm{P(2)-P(4)}}$ (80.6 Hz) is significantly larger than any of the cis couplings in this molecule, consistent with a significant interaction between P(2) and P(4) through the Ru–Co bond *trans* to both ligands; (iii) of the remaining $^2J_{\mathrm{P-P}}$ values all of which are cis couplings, the largest is $^2J_{\mathrm{P(1)-P(4)}}$ (39.7 Hz) between the cobalt coordinated phosphite and the bridging phosphorus nucleus and the smallest $^2J_{\mathrm{P(1)-P(2)}}$ of 11.5 Hz. For the compounds of type **3** (L = phosphine) no cis coupling between the μ-PPh$_2$ group and equatorial phosphines was observable. These results are in agreement with the fact that P–P couplings to phosphite ligands are invariably larger than those to phosphines probably as a result of increased "s" character in the M–P (phosphite) bonds.

Acknowledgment. We are grateful to the Natural Sciences and Engineering Research Council of Canada for operating grants (to A.J.C.) and for funds to support a 3-month visit of S.G. to Waterloo and the University of Rennes for a "Professeur Invitê" position (1 month) to A.J.C. Thanks are also due to C. Roger (Bruker Spectrospin Canada) for recording the ^{31}P spectrum of 4 at 121.5 MHz.

Registry No. 1, 82544-75-0; **2a**, 103533-71-7; **2b**, 103617-40-9; **3a**, 103533-72-8; 4, 103533-73-9; Co, 7440-48-4; Ru, 7440-18-8.

Supplementary Material Available: A table of thermal parameters (1 page); a listing of structure factor amplitudes (22 pages). Ordering information is given on any current masthead page.

---

(19) (a) MacLaughlin, S. A.; Randall, L.; Carty, A. J., unpublished results. (b) Carty, A. J. *Adv. Chem. Ser.* 1981, *No. 196*, 163.

Oxidative-Addition and Proton-Transfer Reactions of Fluorocarbon Acids. Structures of *trans*-(Ph$_3$P)$_2$Pt(H$_2$O)(PhC=CHPh)$^+$HC(SO$_2$CF$_3$)$_2^-$ and *trans*-(Ph$_3$P)$_2$PtH[C-HC(SO$_2$CF$_3$)$_2$][†]

A. R. Siedle,* W. B. Gleason, and R. A. Newmark

Science Research Laboratory, 3M Central Research Laboratories, St. Paul, Minnesota 55144

L. H. Pignolet

Chemistry Department, University of Minnesota, Minneapolis, Minnesota 55455

Received February 6, 1986

Oxidative addition of H$_2$C(SO$_2$CF$_3$)$_2$ to (Ph$_3$P)$_2$Pt(PhC≡CPh) yields the *trans*-diphenylvinyl compound *trans*-(Ph$_3$P)$_2$Pt(*trans*-PhC=CHPh)[C-HC(SO$_2$CF$_3$)$_2$] in which restricted rotation about the Pt–HC(SO$_2$CF$_3$)$_2$ bond has been characterized by ^{31}P DNMR spectroscopy. Recrystallization in air from isopropyl alcohol affords *trans*-(Ph$_3$P)$_2$Pt(*trans*-PhC=CHPh)(H$_2$O)$^+$HC(SO$_2$CF$_3$)$_2^-$: $P2_1/n$, monoclinic, $a = 12.478$ (5) Å, $b = 18.935$ (5) Å, $c = 21.891$ (4) Å, $\beta = 100.43$ (2)°, $R = 0.053$. Oxidative addition of H$_2$C(SO$_2$CF$_3$)$_2$ to (Ph$_3$P)$_2$Pt(C$_2$H$_4$) forms (Ph$_3$P)$_2$PtH[C-HC(SO$_2$CF$_3$)$_2$]: $P2_1/c$, monoclinic, $a = 17.555$ (2) Å, $b = 13.650$ (1) Å, $c = 17.880$ (3) Å, $\beta = 112.70$ (1)°, $R = 0.038$. Analysis of the structural data reveals H$_2$C(SO$_2$CF$_3$)$_2$ to be a large, highly hindered carbon acid, and it is probable that steric effects contribute to the tendency of HC(SO$_2$CF$_3$)$_2^-$ to exist as an anion rather than coordinate to electron-deficient metal centers following proton transfer.

Introduction

We have previously outlined the organometallic chemistry of fluorocarbon acids of the type RHC(SO$_2$CF$_3$)$_2$ (R = H, Ph).[1] These acids possess an unusual collection of properties in that they are strong, nonhygroscopic, nonoxidizing protic acids whose conjugate bases have been shown[2] to coordinate to transition metals, via the central,

---

[†] The C-HC(SO$_2$CF$_3$)$_2$ formulation indicates that the CH(SO$_2$CF$_3$)$_2$ group is bonded to Pt via the methine carbon atom.

(1) Siedle, A. R.; Newmark, R. A.; Pignolet, L. H.; Howells, R. D. *J. Am. Chem. Soc.* 1984, *106*, 1510.

© 1986 American Chemical Society